Extremophiles (2011) 15:587–596
DOI 10.1007/s00792-011-0389-9

ORIGINAL PAPER

The relationship between a coiled morphology and Mbl in alkaliphilic *Bacillus halodurans* C-125 at neutral pH values

Shun Fujinami · Takako Sato · Masahiro Ito

Received: 7 December 2010 / Accepted: 4 July 2011 / Published online: 24 July 2011

Abstract The facultative alkaliphilic *Bacillus halodurans* C-125 can grow in a pH range from 6.8 to 10.8. The morphology of the cells grown at pH values above 7.5 is rod shaped, whereas, that gown at pH values less than 7.5 is coiled. Cytoplasmic membrane staining revealed that this coiled morphology was formed not by one filamentous cell, but by many chained bent/non-bent cells. Prokaryotic actin and tubulin homologs (MreB, Mbl MreBH, and FtsZ, respectively) are known to function as bacterial cytoskeleton proteins. The transcription levels of *ftsZ*, *mreB,* and *mreBH* genes were hardly affected by growth pH. However, the level of the *mbl* gene was significantly decreased at neutral pH values. Moreover, the expression level of the Mbl protein at pH 7.0 was about one-fourth of that at pH 10. Immunofluorescence microscopy (IFM) showed that the Mbl protein was localized as a helical structure in the rod-shaped cell grown at pH 10, whereas a helical structure was not observed in the cells grown at pH 7.0. Fluorescent vancomycin staining showed insertion of new peptidoglycan strands of sidewalls occurred in the cells grown at pH 7.0. These data suggested that a decrease in the expression level of the Mbl protein can influence the morphology of *B. halodurans* C-125 grown at pH 7.0 without influencing insertion of new peptidoglycan strands.

Keywords Alkaliphiles · *Bacillus halodurans* C-125 · Bacterial cytoskeleton · Morphology

Abbreviation
IFM Immunofluorescence microscopy

Introduction

The facultative alkaliphilic *Bacillus halodurans* C-125 (JCM9153) was isolated as a β-galactosidase and xylanase producer in 1977 (Ikura and Horikoshi 1979). The whole genome sequence of *B. halodurans* was completed in 2000 by Takami et al. The strain can grow well in a pH range from 6.8 to 10.8 (Aono 1995). It was reported that the morphology of the cells at logarithmic phase was typically rod shaped at pH values above 7.5 and coiled at pH values less than 7.5 (Aono 1995). A detailed study of such coiled morphology under the neutral pH environment was not reported.

In rod-shaped bacteria, mutations affecting the synthesis or the structure of peptidoglycan (Signoretto et al. 1996; Henriques et al. 1998; Carballido-Lopez and Formstone 2007; Matteï et al. 2010) or loss of teichoic acid (Pooley et al. 1992; Bhavsar et al. 2001) results in abnormal morphology, and the purified cell wall maintains the original rod shape (Holtje 1998). Therefore, the bacterial external peptidoglycan cell wall was traditionally assumed to be

Communicated by A. Oren.

S. Fujinami (✉) · M. Ito
Bio-Nano Electronics Research Centre, Toyo University,
2100 Kujirai, Kawagoe, Saitama 350-8585, Japan
e-mail: s-fujinami@toyo.jp

T. Sato
Marine Biodiversity Research Program,
Institute of Biogeosciences (Biogeos),
Japan Agency for Marine-Earth Science
and Technology (JAMSTEC), 2-15 Natsushima-cho,
Yokosuka, Kanagawa 237-0061, Japan

M. Ito
Faculty of Life Sciences, Toyo University, 1-1-1 Izumino,
Itakura, Oura-gun, Gunma 374-0193, Japan

critical for the determination of cell shape. The long axis of rod-shaped bacteria is affected by the frequency of cell division, and the inhibition of cell division causes cell filamentation (Beall and Lutkenhaus 1991). The balance between cell division and cell elongation affects the cell shape of rod-shaped bacteria (Lleo et al. 1990; Stewart 2005; Carballido-Lopez and Formstone 2007). It was thought that the dynamic tubulin-like cytoskeleton (cell division protein FtsZ) and actin-like cytoskeleton (MreB family of proteins) orchestrate cell wall synthesis and hydrolysis during cell division and cell elongation, respectively (Carballido-Lopez and Formstone 2007; Stewart 2005). The FtsZ ring, composed of a polymer of the FtsZ protein, is formed at the mid-cell in the earliest stage of cell division (Harry 2001; Bramkamp and van Baarle 2009). It is suggested that the Min system and nucleotide occlusion regulate the positioning of the FtsZ ring, i.e., regulate cell division site selection. It is commonly assumed that MreB isoforms of *Bacillus subtilis* (MreB, Mbl, and MreBH) are critical for determination of the cell shape (Carballido-Lopez and Formstone 2007). These proteins are known to be actin homologs, to form a helical structure in the cell, and affect cell wall synthesis, and the mutations in the genes encoding them led to an altered cell shape or to cell death (Wachi et al. 1987; Jones et al. 2001; van den Ent et al. 2001; Carballido-Lopez and Errington 2003; Carballido-Lopez et al. 2006; Defeu Soufo and Graumann 2006; Formstone and Errington 2005). Thus, the MreB family of proteins is thought to determine cell shape in rod-shaped bacteria by controlling the localization of the enzymes that are involved in the cell wall synthesis. It is believed that MreB is important for determination of cell width (Jones et al. 2001; Formstone and Errington 2005), Mbl affects cell elongation of the long axis (Jones et al. 2001; Daniel and Errington 2003; Carballido-Lopez and Errington 2003), and MreBH controls the autolytic activity of the lateral wall by directing cell wall hydrolase LytE (Carballido-Lopez et al. 2006) in *Bacillus subtilis*. Mbl is believed to control the linear axis by directing helical peptidoglycan synthesis (Daniel and Errington 2003; Kawai et al. 2009); however, helical peptidoglycan synthesis occurs without Mbl (Tiyanont et al. 2006). Partial functional redundancy of the MreB family of proteins was suggested (Kawai et al. 2009), but the respective roles of the MreB family of proteins remain uncertain. The *B. halodurans* C-125 genome has three actin-like cytoskeleton proteins encoded by three genes (*mreB, mbl,* and *mreBH*); it was suggested that *B. halodurans* C-125 has a similar peptidoglycan synthetic and morphologic mechanism to *Bacillus subtilis* (Takami et al. 2000).

We investigated the cause of the coiled morphology of *B. halodurans* C-125 cells incubated under neutral pH values. In *B. halodurans* C-125, the quantities of teichuronic acid and teichuronopeptide in the cell walls increase when cells are grown at alkaline pH (Aono 1985) and are necessary for the growth at alkaline pH (Aono 1995). However, the morphology of *B. halodurans* C-125-90, a mutant lacking teichuronic acid and the polyglutamic acid moiety of teichuronopeptide, was typically rod shaped. Thus, it was thought that teichuronic acid and teichuronopeptide were not necessary for keeping the rod-shaped morphology of *B. halodurans* C-125 (Aono et al. 1995). It was reported that the rate of cross-linking of the peptide moieties of peptidoglycan of wild-type cells grown at neutral pH values falls about 40% compared with that of the cells grown at alkaline pH values (Aono and Sanada 1994). The effect of the cross-linking rate of peptidoglycan on cell morphology was not reported. Moreover, an approach from the study of the bacterial cytoskeleton has not been reported in *B. halodurans* C-125.

In this study, we report gene transcriptions, protein expressions, and cellular localizations of bacterial cytoskeleton components of *B. halodurans* C-125 at different pH conditions. Additionally, we compare the insertion of new peptidoglycan strand sites of cells grown at pH 10 and 7.0 by using fluorescent derivatives of the peptidoglycan-binding antibiotic vancomycin. We discuss the effect of bacterial cytoskeleton and peptidoglycan synthesis on coiled morphology in *B. halodurans* C-125 at neutral pH values.

Materials and methods

Bacterial strain and media

Alkaliphilic *Bacillus halodurans* C-125 wild type was used (Aono et al. 1995). *B. halodurans* C-125 cells were grown in alkaline complex medium (pH 10), neutral complex medium (pH 7.0) (Aono and Ohtani 1990), and alkaline complex medium (pH 8.0). Alkaline complex medium (pH 10) contained 15.5 g of K_2HPO_4, 4.5 g of KH_2PO_4, 0.05 g of $MgSO_4{\cdot}7H_2O$, 0.34 g of citric acid, 5 g of peptone, 2 g of yeast extract, and 5 g of glucose, and 10.6 g of Na_2CO_3; per liter of deionized water. For neutral complex medium (pH 7.0), the pH was modified by adding 11.7 g of NaCl instead of Na_2CO_3. For alkaline complex medium (pH 8.0), the pH was modified by reducing Na_2CO_3 and adding NaCl (Fujinami et al. 2007a). In all media, the final pH was adjusted to the desired pH by the addition of KOH or H_2SO_4 as needed.

Escherichia coli DH5αMCR [F- *mcrAΔ1* (*mrr-hsd RMS-mcrBC*) Φ80*dlacZ* Δ(*lacZYAargF*) *U169 deoR recA1 endA1 supE44 λthi-1 gyr-496 relA1*] (Stratagene) was used as a host cell for cloning. *E. coli* DH5αMCR was grown routinely in LB medium.

Morphological observation of *B. halodurans* C-125 by scanning electron microscopy

B. halodurans C-125 wild type was grown aerobically on alkaline complex medium (pH 10) or neutral complex medium (pH 7.0) overnight at 37°C. One milliliter of culture was then inoculated into 100 ml of fresh alkaline complex medium (pH 10) or neutral complex medium (pH 7.0) and grown aerobically at 37°C. Optical density at 600 nm (OD_{600}) was measured every hour for the construction of growth curves. When the OD_{600} reached 0.5, 10 ml of culture was harvested and washed in chilled 0.9% NaCl. Cells were suspended in 900 µl of 0.9% NaCl, and 100 µl of 25% glutaraldehyde was added. The cells were observed by scanning electron microscopy using a model JSM-6700F field emission scanning electron microscope (JEOL).

Microscopic observation of cytoplasmic membranes of *B. halodurans* C-125 by FM4-64 staining

B. halodurans C-125 wild type was grown on alkaline complex medium (pH 10) or neutral complex medium (pH 7.0) as described above. When the OD_{600} reached 0.5, 1 ml of culture was harvested and FM4-64 (Molecular Probes) was added to the culture to a final concentration of 1 µg ml^{-1}. The microscopic images were obtained by Imaging workstation FW4000 (Leica Geosystems), and processed with Photoshop CS software (Adobe Systems). In each experiment, over 30 cells were assessed with respect to the length of the cells and the cell shape (bent or non-bent). The results shown are the averages of three independent experiments.

RNA extraction and transcription analysis

B. halodurans C-125 wild type was grown on alkaline complex medium (pH 10), alkaline complex medium (pH 8.0) and neutral complex medium (pH 7.0) as described above. When the OD_{600} reached 0.5, cells were harvested. The RNA preparation method described by Igo and Losick (1986) was used. Synthesis of cDNA was also performed using a QuantiTect Reverse transcription Kit (Qiagen). Quantitation of transcripts of selected genes was analyzed by quantitative real-time PCR using SYBER Premix ExtaqII (Takara) and PCR Thermal Cycler Dice mini Model TP800 (Takara). All samples were run in duplicate. Transcription levels of each gene were normalized to the *23S* rRNA gene in each sample. The values were quantitated with the ratio of that of alkaline complex medium (pH 10) as 1.0. All results shown are the averages of three independent experiments. Normalized relative transcription levels were tested for significance with the criteria of a transcription level of either >2.0 or <0.5 and $P < 0.05$.

Plasmids and primers

Primers used in this study are listed in Table 1. The primer sets ftsZ-F1 and ftsZ-R1, mbl-F1 and mbl and R1, 23S-F1 and 23S-R1, mreBH-F1 and mreBH-R1, and mreB-F1 and mreB-R1 were used in quantitative transcription analysis. The primer set Mbl-nde1 and Mbl-sal2 was used to amplify the *mbl* gene fragment. Extra nucleotides that were added to introduce restriction sites are shown underlined. The primer set MG-SEQ5 and T7 promoter primer were used for sequencing. pET21b plasmid (Novagen) used for

Table 1 Primers used in this study

Primer	Sequence (5′–3′)	Accession number	Corresponding sequence (nt)
ftsZ-F1	GCCGTGCCCAACAACAA	BA000004.3	2681453–2681437 (minus)
ftsZ-R1	TCTTCTCCGCTTCTTTCTCCT	BA000004.3	2681370–2681390
mbl-F1:	ACCGCCTCCTCCATCAAA	BA000004.3	3861129–3861112 (minus)
mbl-R1	TTTTCTGCCGTCCGTTCC	BA000004.3	3861026–3861043
23S-F1	AAACCGTGTGATCTACCCATG	BA000004.3	25775–25795
23S-R1	TTCACCCCTACCCACACCTC	BA000004.3	25882–25863 (minus)
mreBH-F1	GACACCGCCAAAGGAAATG	BA000004.3	916965–916983
mreBH-R1	CGGAGCGAAACAAGTGGAA	BA000004.3	917109–917091 (minus)
mreB-F1	TTGTCACGAGCCAGTCCATC	BA000004.3	3144572–3144553 (minus)
mreB-R1	CCTGCCGAACCAATCTCAA	BA000004.3	3144437–3144455
Mbl-nde1	GGAATTCCATATGTTTGGAA GGGATATAGG	BA000004.3	3861639–3861623 (minus)
Mbl-sal2	TGCGGTCGACTATACGAACTTTCTTA CTACTTG	BA000004.3	3860638–3860657
MG-SEQ5	CCAAAAGTAGCAGCGAT TGGAGCG	BA000004.3	3861246–3861222 (minus)

Extra nucleotides that were added to introduce restriction sites are underlined

cloning of the *mbl* gene fragment (Yansura and Henner 1984).

Construction of plasmids

PCR was performed on *B. halodurans* C-125 wild-type chromosomal DNA template with the primer set Mbl-nde1 and Mbl-sal2 to amplify the *mbl* gene. The purified product of this reaction was digested with *Nde*I and *Sal*I, and cloned into *Nde*I and *Xho*I-digested pET21b, yielding pETMbl2. It was verified that the insert of pETMbl2 plasmid was mutation free by sequencing. pETMbl2 was used for the production of an anti-Mbl antibody.

Antibodies

pETMbl2 plasmid was sent to Human Combinatiorial Monoclonal Antibody Service (Gene frontier) and yielded a His-tagged Fab-dHLX-MH anti-Mbl recombinant monoclonal antibody (AbyD02867). A rabbit anti-*Shewanella violacea*-FtsZ antibody was used to detect FtsZ of *Bacillus halodurans* C-125. For secondary antibody for Western blot analysis, Goat anti-Rabbit HRP (Bio-Rad) and penta-His HRP conjugate were used. For secondary antibody for immunofluorescence microscopy (IFM), Alexa Fluor 546 goat anti-rabbit IgG (Molecular Probes) and penta-His Alexa Fluor 488 conjugate (QIAGEN) were used.

Western blot analysis of FtsZ and Mbl

B. halodurans C-125 wild type was grown on alkaline complex medium (pH 10) and neutral complex medium (pH 7.0) as described above. When the OD_{600} reached 0.5, cells were harvested and washed in TSE buffer (50 mM Tris–HCl, pH 8.0, 10% sucrose, 1 mM EDTA). Cells were suspended in the same buffer and a protease inhibitor cocktail (SIGMA) was added. Cells were disrupted by sonication and unbroken cells were removed by centrifugation at 9100*g* for 15 min at 4°C. The protein concentration of the broken cell suspension was measured by the Lowry method (Lowry et al. 1951) with BSA as a standard. After the same volume of SDS loading buffer was added and boiled for 3 min at 100°C, samples were separated by 10% polyacrylamide SDS gels (Schagger and von Jagow 1987). After electrophoresis, gels were transferred to nitrocellulose filters (Bio-Rad) electrophoretically overnight in a standard Tris–glycine–methanol buffer.

The following antibodies and reagents were used for detection in Western blot analyses: for FtsZ, 1/3000 rabbit anti-*Shewanella violacea*-FtsZ antibody and 1/3000 Goat anti-Rabbit HRP (Bio-Rad); and for Mbl, 1/1000 His-tagged Fab-dHLX-MH anti-Mbl recombinant monoclonal antibody, 1/3000 penta-His HRP conjugate (QIAGEN). Detection and analyses of chemiluminescence images were conducted using the ECL Plus Western Blotting Detection Reagents (Amersham Biosciences) and the quantitative imaging system Fluor-S MAX (Bio-Rad) according to the protocol provided in the manufacturer's instructions. The relative FtsZ or Mbl content in the crude extracts was calculated from the volume of chemiluminescence of each band. The values were ascertained with the ratio of that of alkaline complex medium (pH 10) as 1.0. All results shown are the averages of three independent experiments.

Immunofluorescence microscopy (IFM)

B. halodurans C-125 wild type was grown on alkaline complex medium (pH 10) and neutral complex medium (pH 7.0) as described above. The fixation method described by Harry et al. (1995) was adapted for *B. halodurans* C-125. When the OD_{600} reached 0.5, 0.5 ml of culture was briefly added to 0.5 ml of glutaraldehyde solution (5% in 60 mM Na-PO_4 buffer, pH 7.5). The cells were fixed for 10 min at room temperature and 45 min on ice. The fixed cells were harvested by centrifugation (700*g* for 15 min at 4°C) and washed in PBS buffer (8 g of NaCl, 0.2 g of KCl, 1.44 g of Na_2HPO_4, 0.24 g of KH_2PO_4; per liter of deionized water) 3 times. Cells were suspended in 0.5 ml of GTE buffer (50 mM glucose, 20 mM Tris–HCl, pH 7.5, 10 mM EDTA).

The Immunofluorescence microscopy (IFM) method described by Fujinami et al. (2007b) was adapted for *B. halodurans* C-125. A glass slide, S-2215 (Matsunami Glass), was covered by 20 µl of poly-L-lysine hydrobromide (1 mg ml^{-1}) and left for 5 min, washed with distilled water, and air dried; 10 µl of the fixed cell suspension was then dropped on the poly-L-lysine coated slide and air dried for 20 min. The slide was covered with 100 µl of lysozyme solution (2 mg/ml in 25 mM Tris–HCl, pH 8.0, 50 mM glucose, 10 mM EDTA) and incubated for 7 min at room temperature. The slide was washed with 5 ml PBSTE (140 mM NaCl, 2 mM KCl, 8 mM Na_2HPO_4, 1.5 mM KH_2PO_4, 0.05% Tween 20, 10 mM EDTA, pH 8) 3 times and then incubated with PBSTE-BSA (PBSTE containing 2% bovine serum albumin) for 15 min at room temperature. The slide was treated for 1 h at room temperature with the primary antibody solution (1/1000 rabbit anti-*Shewanella violacea*-FtsZ antibody for FtsZ and 1/2000 His-tagged Fab-dHLX-MH anti-Mbl recombinant monoclonal antibody for Mbl in PBSTE-BSA), and covered with a cover glass in a shaded moisture chamber. The slide was washed with 5 ml of PBSTE 3 times (the cover glass was removed by washing). After the slide was washed with PBSTE, it was again incubated with PBSTE-BSA for 15 min at room temperature. It was then treated for 1 h at room temperature with a secondary antibody solution

(1/1000 Alexa Fluor 546 goat anti-rabbit IgG (Molecular Probes) for FtsZ, 1/1000 penta-His Alexa Fluor 488 conjugate (QIAGEN) for Mbl in PBSTE-BSA). The slide was then covered with a cover glass in a shaded moisture chamber and was again washed with 5 ml of PBSTE 3 times. After washing with PBSTE, it was covered with a cover glass and sealed with enamel. The microscopic images were obtained by Imaging workstation FW4000 (Leica Geosystems), and processed with Photoshop CS software (Adobe Systems).

Staining with fluorescent vancomycin

B. halodurans C-125 wild type was grown on alkaline complex medium (pH 10) and neutral complex medium (pH 7.0) as described above. The fluorescent vancomycin staining method described by Tiyanont et al. (2006) was used. When the OD_{600} reached 0.5, 1 ml of culture was harvested and incubated with probe solution (1:1 mixture of vancomycin (Wako Pure Chemicals) and the fluorescent BODIPY FL conjugate of vancomycin (VanFL; Molecular Probes), at a final concentration of 0.4 μg/ml each) in 1 ml of PBS buffer for 5 min, and then washed three times with PBS buffer. Cells were spotted on the poly-L-lysine coated glass slide and covered with a cover glass. The microscopic images were obtained by Imaging workstation FW4000 (Leica Geosystems) and processed with Photoshop CS software (Adobe Systems).

Results

The coiled morphology of alkaliphilic *Bacillus halodurans* C-125 grown at pH 7.0 was formed not by one filamentous cell, but by many chained bent/non-bent cells.

The facultative alkaliphilic *Bacillus halodurans* C-125 cells were grown aerobically at pH 10 and 7.0, and growth curves were constructed (Fig. 1). The doubling times are 55.7 ± 4.4 min at pH 10, and 70.7 ± 6.1 min at pH 7.0, respectively. The final optical densities are 1.64 ± 0.21 at pH 10, and 1.60 ± 0.19 at pH 7.0. *B. halodurans* C-125 grown at pH 7.0 showed a slower doubling time and longer lag phase, but the final optical density was not affected.

The morphology of alkaliphilic *Bacillus halodurans* C-125 cells at logarithmic phase was analyzed by scanning electron microscopy (Fig. 2). The morphology of the cells grown at pH 10 is typically rod shaped while, on the other hand, that at pH 7.0 is coiled. This coiled morphology seemed to be composed not by one filamentous cell, but by many chained bent/non-bent cells. To confirm this, the cytoplasmic membrane of *B. halodurans* C-125 was observed after FM4-64 staining (Fig. 3). The cytoplasmic membrane was observed in cells grown at pH 10. The cytoplasmic membrane was also observed in chained bent/non-bent cells grown at pH 7.0. The average lengths of the cells were 3.4 ± 0.58 μm at pH 7.0 and 3.8 ± 0.72 μm at pH 10. The cells grown at pH 7.0 were not filamentous. However, there are two separate subpopulations in a

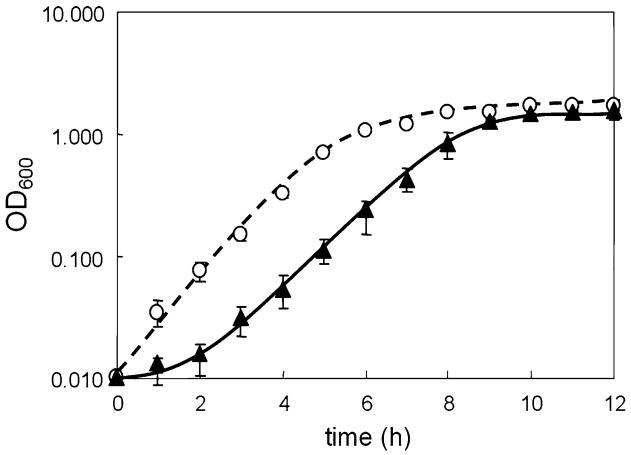

Fig. 1 Growth curve of *B. halodurans* C-125 grown at pH 10 or 7.0. *B. halodurans* C-125 was grown at pH 10 or 7.0. OD_{600} was measured every hour for the construction of growth curves. *Dashed line* and *open circles* show data for pH 10, *solid line* and *filled triangles* show data for pH 7.0. All results shown are the averages of three independent experiments

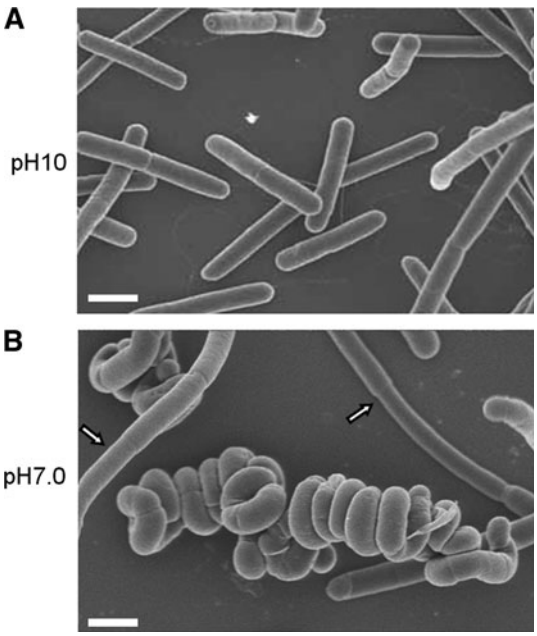

Fig. 2 Morphological observation of *B. halodurans* C-125 grown at pH 10 or 7.0 by scanning electron microscopy. *B. halodurans* C-125 was grown at pH 10 or 7.0. The cells were observed by scanning electron microscopy. Photomicrograph of *B. halodurans* C-125 grown at pH 10 (**a**) or 7.0 (**b**). There are two separate subpopulations (bent and non-bent cells) in a culture at pH 7.0. Non-bent cells are shown by the *arrows*. All photographs are of the same magnification. The *bar* represents 1 μm

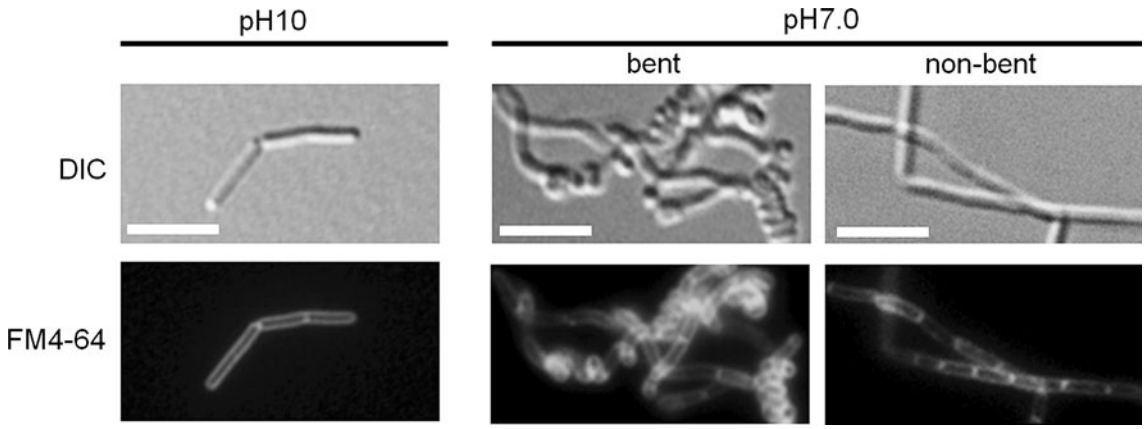

Fig. 3 Microscopic observation of the cytoplasmic membrane of *B. halodurans* C-125 grown at pH 10 or 7.0. *B. halodurans* C-125 was grown at pH 10 or 7.0. The cytoplasmic membrane was stained by FM4-64, and observed by fluorescence microscopy. The rod-shaped cell grown at pH 10, bent cell grown at pH 7.0, and non-bent cell grown at pH 7.0 are shown. The image analyses are indicated at the *left*; DIC, differential-interference contrast microscopy; FM4-64, fluorescence microscopy for cytoplasmic membrane stained by FM4-64. All Photographs are of the same magnification. The *bar* represents 5 μm

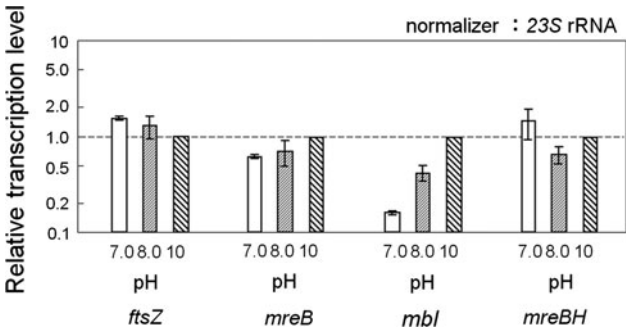

Fig. 4 Transcription analysis of cytoskeleton genes of *B. halodurans* C-125 grown at pH 7.0, 8.0, or 10. *B. halodurans* C-125 was grown at pH 7.0, 8.0, or 10. Quantitation of transcripts of *ftsZ, mreB, mbl,* and *mreBH* genes were analyzed by quantitative real-time PCR. Primers are listed in Table 1. All samples were run in duplicate. Transcription levels of each gene were normalized to the *23S* rRNA gene in each sample. The transcription levels presented are relative to the levels in cells grown at pH 10 (that is set as 1.0). All results shown are the averages of three independent experiments

culture at pH 7.0: 42.1 ± 2.0% of 'bent' cells and 57.9 ± 2.0% of 'non bent' cells. The transcription levels of *ftsZ, mreB,* and *mreBH* gene were not affected by growth pH, but that of the *mbl* gene was decreased at neutral pH value.

To investigate the effect of growth pH conditions on the transcription level of bacterial cytoskeleton genes (*ftsZ, mreB, mbl* and *mreBH*), quantitative real-time PCR analyses were carried out on cDNA of *B. halodurans* C-125 that had been grown at pH 7.0, 8.0, or 10 (Fig. 4). The transcription levels of *ftsZ, mreB,* and *mreBH* were hardly affected by growth pH. However, that of *mbl* was affected by growth pH, especially at pH 7.0. The transcription level of *mbl* at pH 7.0 was about one-fifth of that at pH 10. The expression level of FtsZ was not affected by growth pH, but that of Mbl was decreased at neutral pH value.

In this study, we have made an anti-Mbl recombinant monoclonal antibody (see "Materials and methods"). Western blot analyses using anti-Mbl antibody were carried out on whole-cell crude extract of *E. coli* C41 (DE3) transformed with either pDH88 (a plasmid with an IPTG-inducible P*spac* promoter) or pDHMbl1 (*mbl* was inserted into pDH88) that had been induced with IPTG. The single bands in expected positions of Mbl were detected only in whole cell crude extract of *E. coli* C41 (DE3) transformed with pDHMbl (data not shown). This antibody has been used in the following experiments.

To investigate the effect of growth pH conditions on the expression level of tubulin-like cell division protein FtsZ and actin-like cytoskeleton protein Mbl, Western blot analyses using a rabbit anti-*Shewanella violacea*-FtsZ antibody and an anti-Mbl recombinant monoclonal antibody were carried out on whole cell crude extracts of *B. halodurans* C-125 grown at pH 7.0 and 10 (Fig. 5). Using a rabbit anti-*Shewanella violacea*-FtsZ antibody, a single band was detected at the position of about 41 kDa in each lane, corresponding to the size of FtsZ (Fig. 5a). Using anti-Mbl recombinant monoclonal antibody, a single band was detected at the position of about 36 kDa in each lane, corresponding to the size of Mbl (Fig. 5b). The relative expression levels were estimated from the intensity of chemiluminescence of each band. The expression level of FtsZ was not affected by growth pH (pH 7.0 or 10). The expression level of Mbl at pH 7.0 was about one-fourth of that at pH 10. Clear localization of Mbl was not observed in the cells grown at pH 7.0, while localization of FtsZ was observed.

To investigate the effect of growth pH conditions on the subcellular localization of FtsZ and Mbl, immunofluorescence microscopy (IFM) was carried out on glutaraldehyde

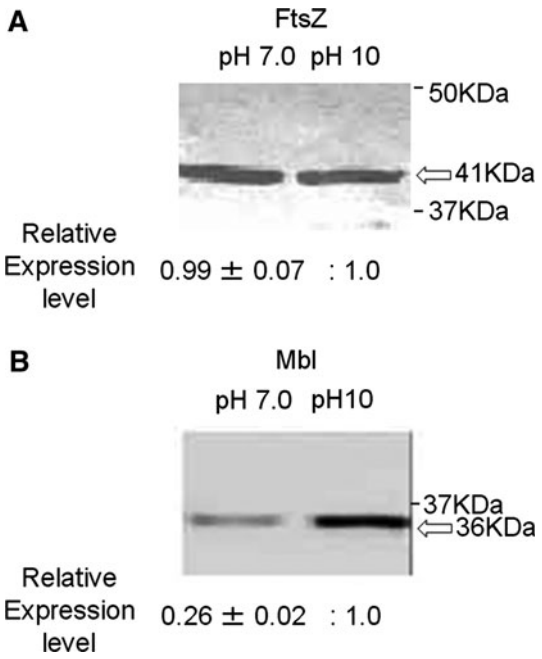

Fig. 5 Western blot analysis of FtsZ or Mbl of *B. halodurans* C-125 grown at pH 10 or 7.0. *B. halodurans* C-125 was grown at pH 10 or 7.0. Western blot analyses using antibodies against FtsZ (**a**) or Mbl (**b**) were performed. The positions of about 41- and 36-KDa proteins, corresponding to the size of FtsZ and Mbl, are shown by the *arrow*. The *numbers* under the bands are the expression levels, presented relative to the level in cells grown at pH 10 (that is set as 1.0). The values are the averages of three independent experiments

fixed cells of *B. halodurans* C-125 that had been grown at pH 7.0 or 10 (Fig. 6).

Tubulin-like cell division protein FtsZ was localized at the center and/or pole of the cells grown at pH 10. Such subcellular localization of FtsZ was also seen in each of the bent/non-bent cells grown at pH 7.0. The subcellular localization of FtsZ was not affected by growth pH.

Actin-like cytoskeleton protein Mbl was localized as a helical structure in the rod-shaped cells at pH 10. However, the helical structure of Mbl was hardly observed in the cells grown at pH 7.0, either in bent or non- bent cells. Helical peptidoglycan synthesis was observed in chained bent/non-bent cells at pH 7.0.

To investigate the insertion of new peptidoglycan strands in *B. halodurans* C-125, we compared the staining patterns observed in the cells grown at pH 7.0 or 10 using fluorescent derivatives of the PG-binding antibiotic vancomycin (Fig. 7). Bright signals were observed at mid-cell and the poles of the rod-shaped cells grown at pH 10 and also chained bent/non-bent cells grown at pH 7.0. Helical staining patterns along the cylindrical walls were also observed in rod-shaped cells grown at pH 10 and non-bent cells grown at pH 7.0. However, the helical staining patterns were not clear in bent cells compared with non-bent cells.

Discussion

Here, we report the detailed morphology of *B. halodurans* C-125 cells grown at pH 10 and 7.0. The morphology of the cells grown at pH 10 is standard rod shaped while, on the other hand, the cells grown at pH 7.0 are coiled (Aono 1995, Fig. 2). Cytoplasmic membrane staining revealed that this coiled morphology is formed not by one filamentous cell, but by many chained bent/non-bent cells (Fig. 3).

FtsZ is a tubulin-like cell division protein that forms the FtsZ ring to direct septation at the cell division site (Harry 2001, Bramkamp and van Baarle 2009), and an *ftsZ* mutant of *Bacillus subtilis* showed a filamentous shape (Beall and Lutkenhaus 1991). Therefore, we analyzed the transcription level of the *ftsZ* gene (Fig. 4), the expression level of FtsZ protein (Fig. 5a), and subcellular localization of the FtsZ ring (Fig. 6). They were not affected by culture pH. The cytoplasmic membrane was observed in chained bent/non-bent cells grown at pH 7.0 (Fig. 3). The measurement of cell lengths showed that the cells grown at pH 7.0 were not filamentous. These results strongly suggested that cell division occurred in chained bent/non-bent cells of *B. halodurans* C-125 grown at pH 7.0.

It was reported that bacterial cytoskeletons play an important role in cell shape formation and cell wall synthesis of rod-shaped bacteria including *Bacillus* species (Jones et al. 2001; van den Ent et al. 2001, Carballido-Lopez and Errington 2003; Carballido-Lopez et al. 2006; Formstone and Errington 2005; Defeu Soufo and Graumann 2006). Therefore, we focused on actin-like bacterial cytoskeletal proteins. The *B. halodurans* C-125 genome encodes three actin-like cytoskeleton protein encoding genes, *mreB, mbl*, and *mreBH*. We compared transcription levels of these three bacterial cytoskeleton genes at pH values of 7.0, 8.0, and 10 (Fig. 4). The transcription levels of the *mreB* and *mreBH* genes were hardly affected by growth pH. However, the transcription level of the *mbl* gene at pH 7.0 was about one-fifth of that at pH 10. The results confirmed the report that transcription of the *mbl* gene of *B. halodurans* C-125 is strongly up-regulated under the alkaline pH environment, but not *mreB* and *mreBH* (Annual report of JAMSTEC JAMSTEC 2003). The expression level of Mbl at pH 7.0 was about one-fourth of that at pH 10 (Fig. 5b). Mbl was localized as a helical structure in the rod-shaped cell at pH 10 (Fig. 6). This was in agreement with the report for *B. subtilis* (Jones et al. 2001). However, the helical structure of Mbl was not observed in the cells grown at pH 7.0 (Fig. 6). These results suggested that the decrease of *mbl* gene transcription causes a decrease of Mbl protein expression and disruption of subcellular localization in the cells grown at pH 7.0.

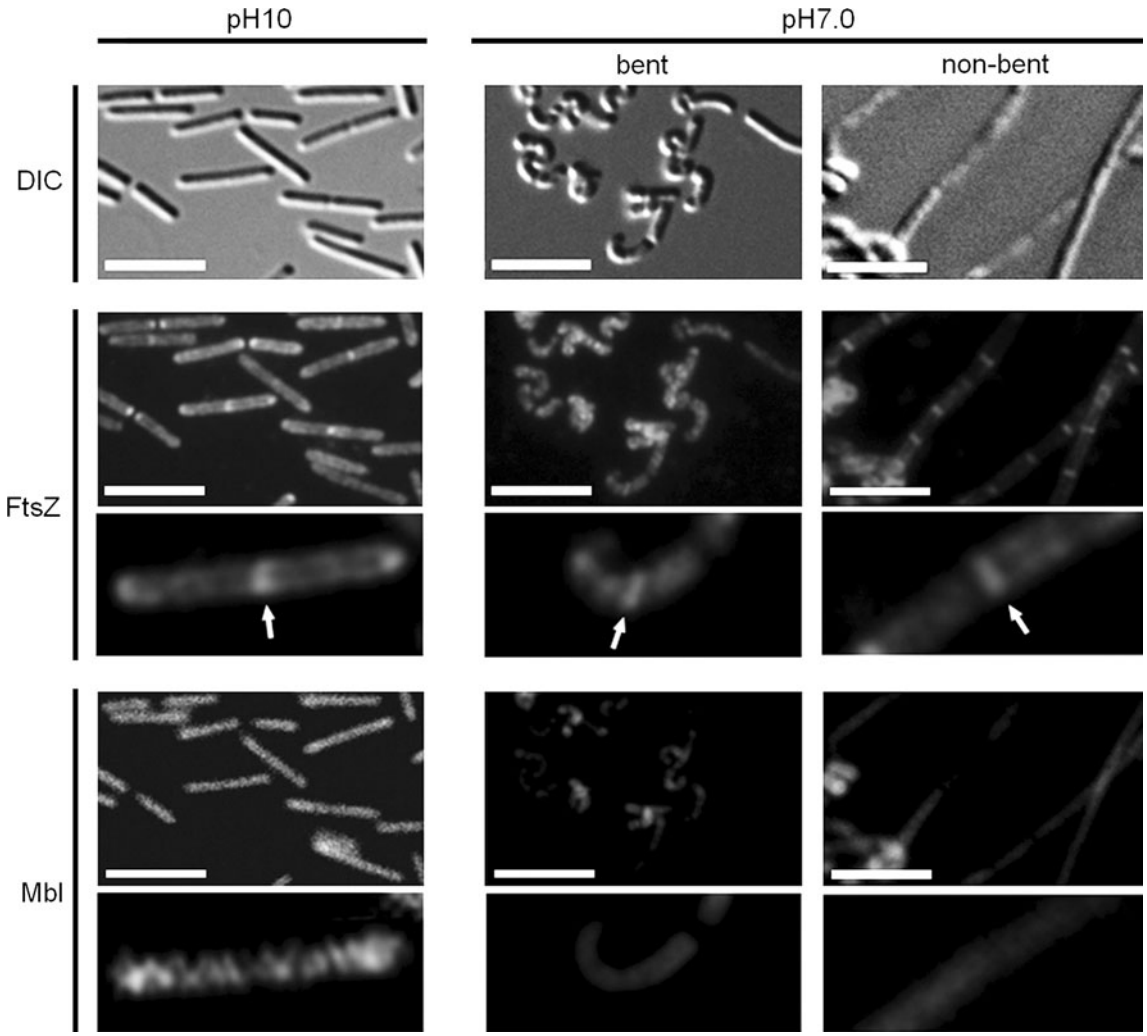

Fig. 6 Immunofluorescence microscopy analyses of the subcellular localization of FtsZ and Mbl in *B. halodurans* C-125. *B. halodurans* C-125 was grown aerobically at pH 10 or 7.0. The subcellular localization of FtsZ and Mbl were visualized by Immunofluorescence microscopy (IFM). The rod-shaped cells grown at pH 10, bent cells grown at pH 7.0, and non-bent cells grown at pH 7.0 are shown. The image analyses are indicated at the *left*; DIC, differential-interference contrast microscopy; FtsZ, immunofluorescence microscopy for FtsZ; Mbl, immunofluorescence microscopy for Mbl. The *bar* represents 5 μm. An enlarged image is shown at the *bottom*. The subcellular localization of FtsZ is shown by the *arrow*

The method of disrupting a target gene on the chromosome of *B. halodurans* C-125 has not been established, thus we attempted to construct an *mbl* mutant of *B. halodurans* C-125 by referring to the high-efficiency gene inactivation and replacement system (Biswas et al. 1993) used in related alkaliphilic *B. pseudofirmus* OF4 (Fujinami et al. 2007a). However, an *mbl* mutant of *B. halodurans* C-125 was not obtained. In *B. subtilis*, it was reported that viable, non-suppressed *mbl* mutants can be obtained in the presence of high concentrations of magnesium (Schirner and Errington 2009). We also tried a medium with high concentration of magnesium, but an *mbl* mutant of *B. halodurans* C-125 was not obtained.

We also investigated the insertion of new peptidoglycan strands in *B. halodurans* C-125 by using fluorescent vancomycin. Bright mid-cell staining and helical side wall staining were observed in *B. halodurans* C-125 grown at pH 10. This was in agreement with the report for *B. subtilis* (Daniel and Errington 2003; Tiyanont et al. 2006). Similar staining was observed in the cells grown at pH 7.0 with reduced Mbl protein expression levels. Several years ago, it was reported that sidewall staining was observed in both *mbl*-deficient and wild-type cells of *Bacillus subtilis* (Tiyanont et al. 2006). Redundant functions of MreB family proteins were suggested in cell morphogenesis (Kawai et al. 2009), and other cytoskeleton proteins may control the biosynthesis of peptidoglycan. It was concluded that the insertion of new peptidoglycan strands occurred in *B. halodurans* C-125 cells grown at neutral pH value without the Mbl protein. The helical staining patterns were

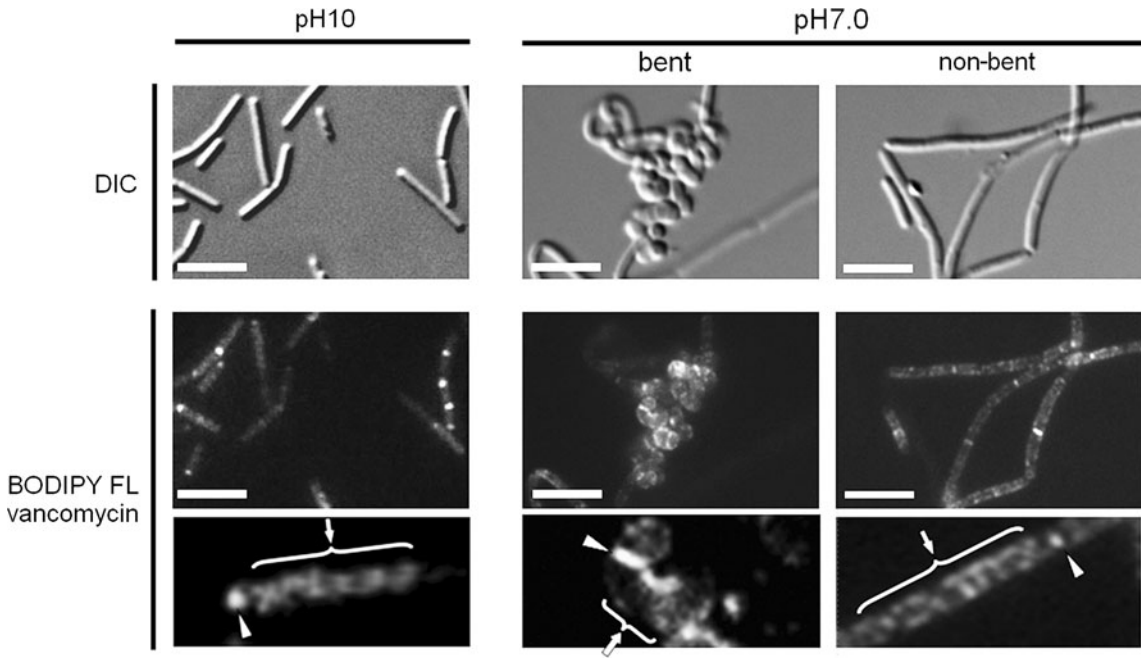

Fig. 7 Staining of *B. halodurans* C-125 cells grown at pH 7.0 with fluorescent vancomycin. *B. halodurans* C-125 was grown at pH 10 or 7.0. The fluorescent vancomycin solution (1:1 mixture of vancomycin (Wako) and the fluorescent BODIPY FL conjugate of vancomycin (VanFL; Molecular Probes), at a final concentration of 0.4 μg/ml each) were used for the staining of insertion of new peptidoglycan strands. Rod-shaped cells grown at pH 10, bent cells grown at pH 7.0, and non-bent cells grown at pH 7.0 are shown. The image analyses are indicated at the *left*; DIC, differential-interference contrast microscopy; BODIPY FL vancomycin, fluorescent vancomycin staining. The *bar* represents 5 μm. Enlarged images are shown at the *bottom*. The bright signals at mid-cell and at the poles of the cell are shown by the *arrowhead*. Helical staining patterns along the cylindrical walls are shown by the *bracketed arrow*

not clear in bent cells compared with non-bent cells. This suggests the difficulty of focusing on cells arranged in three dimensions or the possibility that some difficulty in helical insertion of new peptidoglycan occurred in bent cells.

It was reported that the rate of cross-linking of the peptide moieties of peptidoglycan of *B. halodurans* C-125 grown at pH 7.0 was lower than that grown at pH 10 (Aono and Sanada 1994). In *B. halodurans* C-125, the activity or subcellular localization of an enzyme catalyzing the cross-linking of peptidoglycan, such as Ldt (Magnet et al. 2007), may be affected at neutral pH value. In *Helicobacter pylori*, peptidoglycan cross-linking relaxation promotes helical cell shape (Sycuro et al. 2010), and thus a decreased rate of cross-linking may cause bent cells in *B. halodurans* C-125.

The cause of the chained morphology of *B. halodurans* C-125 cells grown at pH 7.0 is still unknown. A possibility is that expression level or catalytic activity or localization of an enzyme which is involved in the cell separation after cell division, such as CwlS (Fukushima et al. 2006), may decrease under a neutral pH environment. Future studies will explore whether Mbl protein affects the localization of these enzymes.

Acknowledgments We are grateful to Dr. Arthur A. Guffanti for critical reading of the manuscript and for helpful suggestions, Dr. Katsuyuki Uematsu for assistance with morphological observation by scanning electron microscopy, and Mr. Takahiro Tomomatsu for technical assistance. This work was supported by a grant from Bio-Nano Electronics Research Centre, Toyo University (to M.I.).

References

Aono R (1985) Isolation and partial characterization of structural components of the walls of alkalophilic *Bacillus* strain C-125. J Gen Microbiol 131:105–111

Aono R (1995) assignment of facultatively alkaliphilic *Bacillus* sp. strain C-125 to *Bacillus lentus* Group 3. Int J Syst Bacteriol 45:582–585

Aono R, Ohtani M (1990) Loss of alkalophily in cell-wall-component-defective mutants derived from alkalophilic *Bacillus* C-125. Isolation and partial characterization of the mutants. Biochem J 266:933–936

Aono R, Sanada T (1994) Hyper-autolysis of the facultative alkalophile *Bacillus* sp. C-125 cells grown at neutral pH: culture-pH dependant cross-linking of the peptide moieties of the peptidoglycan. Biosci Biotechnol Biochem 58:2015–2019

Aono R, Ito M, Joblin K, Horikoshi K (1995) A high cell wall negative charge is necessary for the growth of the alkaliphile *Bacillus lentus* C-125 at elevated pH. Microbiology 141:2955–2964

Beall B, Lutkenhaus J (1991) FtsZ in *Bacillus subtilis* is required for vegetative septation and for asymmetric septation during sporulation. Genes Dev 5:447–455

Bhavsar AP, Beveridge TJ, Brown ED (2001) Precise deletion of *tagD* and controlled depletion of its product, glycerol

3-phosphate cytidylyltransferase, leads to irregular morphology and lysis of *Bacillus subtilis* grown at physiological temperature. J Bacteriol 183:6688–6693

Biswas I, Gruss A, Ehrlich SD, Maguin E (1993) High-efficiency gene inactivation and replacement system for gram-positive bacteria. J Bacteriol 175:3628–3635

Bramkamp M, van Baarle S (2009) Division site selection in rod-shaped bacteria. Curr Opin Microbiol 12:683–688

Carballido-Lopez R, Errington J (2003) The bacterial cytoskeleton: in vivo dynamics of the actin-like protein Mbl of *Bacillus subtilis*. Dev Cell 4:19–28

Carballido-Lopez R, Formstone A (2007) Shape determination in *Bacillus subtilis*. Curr Opin Microbiol 10:611–616

Carballido-Lopez R, Formstone A, Li Y, Ehrlich SD, Noirot P, Errington J (2006) Actin homolog MreBH governs cell morphogenesis by localization of the cell wall hydrolase LytE. Dev Cell 11:399–409

Daniel RA, Errington J (2003) Control of cell morphogenesis in bacteria: two distinct ways to make a rod-shaped cell. Cell 113:767–776

Defeu Soufo HJ, Graumann PL (2006) Dynamic localization and interaction with other *Bacillus subtilis* actin-like proteins are important for the function of MreB. Mol Microbiol 62:1340–1356

Formstone A, Errington J (2005) A magnesium-dependent *mreB* null mutant: implications for the role of *mreB* in *Bacillus subtilis*. Mol Microbiol 55:1646–1657

Fujinami S, Sato T, Trimmer JS, Spiller BW, Clapham DE, Krulwich TA, Kawagishi I, Ito M (2007a) The voltage-gated Na^+ channel Na_VBP co-localizes with methyl-accepting chemotaxis protein at cell poles of alkaliphilic *Bacillus pseudofirmus* OF4. Microbiology 153:4027–4038

Fujinami S, Terahara N, Lee S, Ito M (2007b) Na^+ and flagella-dependent swimming of alkaliphilic *Bacillus pseudofirmus* OF4: a basis for poor motility at low pH and enhancement in viscous media in an "up-motile" variant. Arch Microbiol 187:239–247

Fukushima T, Afkham A, Kurosawa S, Tanabe T, Yamamoto H, Sekiguchi J (2006) A new D, L-endopeptidase gene product, YojL (renamed CwlS), plays a role in cell separation with LytE and LytF in *Bacillus subtilis*. J Bacteriol 188:5541–5550

Harry EJ (2001) Bacterial cell division: regulating Z-ring formation. Mol Microbiol 40:795–803

Harry EJ, Pogliano K, Losick R (1995) Use of immunofluorescence to visualize cell-specific gene expression during sporulation in *Bacillus subtilis*. J Bacteriol 177:3386–3393

Henriques AO, Glaser P, Piggot PJ, Moran CP Jr (1998) Control of cell shape and elongation by the rodA gene in *Bacillus subtilis*. Mol Microbiol 28:235–247

Holtje JV (1998) Growth of the stress-bearing and shape-maintaining murein sacculus of *Escherichia coli*. Microbiol Mol Biol Rev 62:181–203

Igo MM, Losick R (1986) Regulation of a promoter that is utilized by minor forms of RNA polymerase holoenzyme in *Bacillus subtilis*. J Mol Biol 191:615–624

Ikura Y, Horikoshi K (1979) Isolation and some properties of galactosidase producing bacteria. Agric Biol Chem 43:85–88

JAMSTEC (2003) Annual report of JAMSTEC 2002. 76–88, http://www.jamstec.go.jp/pdf/nenpo_pdf/np_h14/2-06.pdf

Jones LJ, Carballido-Lopez R, Errington J (2001) Control of cell shape in bacteria: helical, actin-like filaments in *Bacillus subtilis*. Cell 104:913–922

Kawai Y, Asai K, Errington J (2009) Partial functional redundancy of MreB isoforms, MreB, Mbl and MreBH, in cell morphogenesis of *Bacillus subtilis*. Mol Microbiol 73:719–731

Lleo MM, Canepari P, Satta G (1990) Bacterial cell shape regulation: testing of additional predictions unique to the two-competing-sites model for peptidoglycan assembly and isolation of conditional rod-shaped mutants from some wild-type cocci. J Bacteriol 172:3758–3771

Lowry OH, Rosebrough NJ, Farr AL, Randall RJ (1951) Protein measurement with the Folin phenol reagent. J Biol Chem 193:265–275

Magnet S, Arbeloa A, Mainardi JL, Hugonnet JE, Fourgeaud M, Dubost L, Marie A, Delfosse V, Mayer C, Rice LB, Arthur M (2007) Specificity of L, D-transpeptidases from gram-positive bacteria producing different peptidoglycan chemotypes. J Biol Chem 282:13151–13159

Matteï PJ, Neves D, Dessen A (2010) Bridging cell wall biosynthesis and bacterial morphogenesis. Curr Opin Struct Biol 20:749–755

Pooley HM, Abellan FX, Karamata D (1992) CDP-glycerol:poly-(glycerophosphate) glycerophosphotransferase, which is involved in the synthesis of the major wall teichoic acid in *Bacillus subtilis* 168, is encoded by *tagF* (*rodC*). J Bacteriol 174:646–649

Schagger H, von Jagow G (1987) Tricine-sodium dodecyl sulfate-polyacrylamide gel electrophoresis for the separation of proteins in the range from 1 to 100 kDa. Anal Biochem 166:368–379

Schirner K, Errington J (2009) The cell wall regulator {sigma}I specifically suppresses the lethal phenotype of mbl mutants in *Bacillus subtilis*. J Bacteriol 191:1404–1413

Signoretto C, Di Stefano F, Canepari P (1996) Modified peptidoglycan chemical composition in shape-altered *Escherichia coli*. Microbiology 142(Pt 8):1919–1926

Stewart GC (2005) Taking shape: control of bacterial cell wall biosynthesis. Mol Microbiol 57:1177–1181

Sycuro LK, Pincus Z, Gutierrez KD, Biboy J, Stern CA, Vollmer W, Salama NR (2010) Peptidoglycan crosslinking relaxation promotes *Helicobacter pylori*'s helical shape and stomach colonization. Cell 141:822–833

Takami H, Nakasone K, Takaki Y, Maeno G, Sasaki R, Masui N, Fuji F, Hirama C, Nakamura Y, Ogasawara N, Kuhara S, Horikoshi K (2000) Complete genome sequence of the alkaliphilic bacterium *Bacillus halodurans* and genomic sequence comparison with *Bacillus subtilis*. Nucleic Acids Res 28:4317–4331

Tiyanont K, Doan T, Lazarus MB, Fang X, Rudner DZ, Walker S (2006) Imaging peptidoglycan biosynthesis in *Bacillus subtilis* with fluorescent antibiotics. Proc Natl Acad Sci USA 103:11033–11038

van den Ent F, Amos LA, Lowe J (2001) Prokaryotic origin of the actin cytoskeleton. Nature 413:39–44

Wachi M, Doi M, Tamaki S, Park W, Nakajima-Iijima S, Matsuhashi M (1987) Mutant isolation and molecular cloning of mre genes, which determine cell shape, sensitivity to mecillinam, and amount of penicillin-binding proteins in *Escherichia coli*. J Bacteriol 169:4935–4940

Yansura DG, Henner DJ (1984) Use of the *Escherichia coli* lac repressor and operator to control gene expression in *Bacillus subtilis*. Proc Natl Acad Sci USA 81:439–443